

Simulation study of anisotropic random sequential adsorption of extended objects on a triangular lattice

Lj. Budinski-Petković,¹ I. Lončarević,¹ Z. M. Jakšić,² S. B. Vrhovac,² and N. M. Švrakić²

¹*Faculty of Engineering, Trg D. Obradovića 6, Novi Sad 21000, Serbia*

²*Institute of Physics Belgrade, University of Belgrade, Pregrevica 118, Zemun 11080, Belgrade, Serbia*

(Received 11 July 2011; revised manuscript received 28 September 2011; published 1 November 2011)

The properties of the anisotropic random sequential adsorption (RSA) of objects of various shapes on a two-dimensional triangular lattice are studied numerically by means of Monte Carlo simulations. The depositing objects are formed by self-avoiding lattice steps, whereby the first step determines the orientation of the object. Anisotropy is introduced by positing unequal probabilities for orientation of depositing objects along different directions of the lattice. This probability is equal p or $(1 - p)/2$, depending on whether the randomly chosen orientation is horizontal or not, respectively. Approach of the coverage $\theta(t)$ to the jamming limit θ_{jam} is found to be exponential $\theta_{\text{jam}} - \theta(t) \propto \exp(-t/\sigma)$, for all probabilities p . It was shown that the relaxation time σ increases with the degree of anisotropy in the case of elongated and asymmetrical shapes. However, for rounded and symmetrical shapes, values of σ and θ_{jam} are not affected by the presence of anisotropy. We finally analyze the properties of the anisotropic RSA of polydisperse mixtures of k -mers. Strong dependencies of the parameter σ and the jamming coverage θ_{jam} on the degree of anisotropy are obtained. It is found that anisotropic constraints lead to the increased contribution of the longer k -mers in the total coverage fraction of the mixture.

DOI: [10.1103/PhysRevE.84.051601](https://doi.org/10.1103/PhysRevE.84.051601)

PACS number(s): 68.43.Mn, 05.10.Ln, 02.50.-r, 05.70.Ln

I. INTRODUCTION

Deposition, or adsorption, of extended objects at different surfaces is of considerable interest for a wide range of applications in biology, nanotechnology, device physics, physical chemistry, and materials science [1,2]. Typically, such objects range in size from submicrometer scale down to nanometers, and, depending on the application in question, the objects could be polymers, globular proteins, nanotubes, DNA segments, oligonucleotides, or general geometrical shapes such as discs, polygons, etc. Early studies have focused on deposition of regular shapes on spatially homogeneous, regular substrates [3], but recent interest has shifted to deposition of irregular objects on prepatterned or otherwise structured or inhomogeneous surfaces [4–7]. In real experimental situations these include minerals, pigments, biological membranes, wafers, and other substrates that are inherently heterogeneous. When the patterning scale is comparable to the object size, the underlying pattern alters surface-object interaction, thus imposing modified morphology and dynamics of the deposition process. For instance, patterning of substrates can be used to promote more stable and regular adsorption at desired substrate sites, as in, e.g., DNA arrays [8,9]. Thus, understanding the impact of surface topography and/or heterogeneity is essential for controlling the adsorption process.

Theoretically, several models have been developed to capture the basic physics of this situation, and by far the most studied is that of random sequential adsorption (RSA) [3]. In this model particles (objects) are sequentially deposited on the randomly chosen site of the substrate. When deposited, such objects are irreversibly attached to the site. If the chosen site is already occupied, the deposition is rejected, the particle is discarded, and the deposition is next attempted at a different randomly chosen site. Note that, in this process, particle-particle and particle-substrate interactions are modeled solely by geometrical and other features included in the deposition procedure. Excluded volume, or particle-particle interaction,

is incorporated by rejection of deposition overlap, while the particle-substrate interaction is modeled by the irreversibility of deposition. In real RSA simulations, the substrate is usually modeled by some two-dimensional (2D) regular lattice (array of points) [10]. The kinetic properties of a deposition process are described by the time evolution of the coverage $\theta(t)$, which is the fraction of the substrate area occupied by the adsorbed particles. With this setup, one is typically interested in long-term behavior of the coverage fraction. Specifically, after a sufficiently long time, the deposited layer will reach “jamming limit” when no further deposition of particles is possible. Approach to the jamming coverage with time is known to be asymptotically algebraic for continuum systems [11–14] and exponential for lattice models [15–18]. For the latter case the approach of the coverage fraction to its jamming limit is given by the time dependence:

$$\theta(t) \sim \theta_{\text{jam}} - \Delta\theta \exp(-t/\sigma), \quad (1)$$

where parameters θ_{jam} , $\Delta\theta$, and σ depend on the shape and orientational freedom of depositing objects [17,18].

In order to account for inhomogeneous surfaces in our RSA model, we have introduced *anisotropy* in the deposition procedure. Namely, even when the deposition at a randomly chosen site is allowed, the probability for deposition is different along different directions of the underlying lattice (in this work we consider a triangular lattice as a substrate). This simple modification introduces preferential direction in the deposition process and, depending on the shape of deposited objects, imposes this specific “patterning” on the deposited layer. This is particularly striking in the case when the *mixture* of objects (which we also study) is deposited; anisotropy may favor deposition of one kind over the other.

To the best of our knowledge, there are no reports on the anisotropic RSA of shapes other than dimers on a square lattice. Oliveira *et al.* [19] have studied anisotropic RSA of dimers on a square lattice by Monte Carlo simulation

and the time-series expansion. Interestingly, they reported that the jamming coverage has a discontinuity at vanishing probability of choosing vertical bonds to place a dimer. Recently, percolation and jamming phenomena have been investigated for anisotropic sequential deposition of dimers on a square lattice [20]. In particular, this model is useful for description of isolator-(semi)conductor phase transition upon aligned deposition of the prolate objects on a substrate [21].

Considerable numerical studies have been devoted to the 2D deposition of randomly oriented anisotropic (elliptical and rectangular) particles with both position and orientation sampled from a random distribution [16,22–26]. In these systems, the deposition process evolves in two regimes. During the first stage objects can fall at random, and nearly every adsorption attempt is successful. Thereafter only particles of orientation similar to that of the already deposited particles will successfully adsorb, which slows down the kinetics. This produces an ordering effect and better packing since parallel objects tend to cluster, forming large oriented domains in the jamming limit [16,27].

The effect of size polydispersity on the growth of deposition structures was mainly studied to obtain their jamming limits and their late-time kinetics. Studies include binary mixtures [28–31] and mixtures of particles obeying various (uniform, Gaussian, power-law) size distributions [29,32–34]. Theoretical works were restricted only to binary mixtures of particles with very large size differences [35–37] and mixtures with power-law size distribution of particles [33,38]. It is concluded that the mixtures cover the lattice more efficiently than either of the species separately [36,39]. Recently, more attention has been given to the monolayer growth by several species of different shape and/or size [18,31].






The main goal of the present study is to investigate the interplay between the anisotropy of deposition and the symmetry properties of deposited shapes. This work discusses the rapidity of the approach to the jamming state and the values of the jamming coverages for various degrees of anisotropy of the deposition process. Here we focus our interest on the influence of the order of symmetry axis of the shape on the kinetics of the deposition processes under anisotropic conditions. This work provides for the first time a closer insight into the deposition process of polydisperse mixtures in anisotropic conditions.

The paper is organized as follows. Section II describes the details of the model and simulations. We give the simulation results and discussions for the one-component deposition in Sec. III and for the mixture in Sec. IV. Finally, Sec. V contains some additional comments and final remarks.

II. DEFINITION OF THE MODEL AND THE SIMULATION METHOD

The depositing shapes are modeled by directed self-avoiding walks on a triangular lattice. A self-avoiding shape of length ℓ is a sequence of distinct vertices $(\omega_0, \dots, \omega_\ell)$ such that each vertex is a nearest neighbor of its predecessor; i.e., a walk of length ℓ covers $\ell + 1$ lattice sites. Examples of such walks for $\ell = 1, 2$, and 6 are shown in Table I. On a triangular lattice objects with a symmetry axis of first, second, third, and sixth order can be formed. Rotational symmetry of order n_s , also

TABLE I. Various shapes (x) of length ℓ on a triangular lattice. n_s denotes the order of the symmetry axis of the shape.

(x)	Shape	n_s	ℓ
A		2	1
B		2	2
C		1	2
D		3	2
E		6	6

called n -fold rotational symmetry, with respect to a particular axis perpendicular to the triangular lattice, means that rotation by an angle of $2\pi/n_s$ does not change the object.

At each Monte Carlo step we randomly select a lattice site and try to deposit the shape of length ℓ . If the selected site is occupied by a deposited object, the adsorption attempt is rejected. If the selected site is unoccupied, we fix the beginning of the walk that makes the chosen shape at this site. Anisotropy is introduced by positing unequal rates for deposition of objects in the three possible directions. The choice of the horizontal direction occurs with probability p and for each of the other two directions with probability $(1 - p)/2$. Hence, the value of $p = \frac{1}{3}$ corresponds to the isotropic case. We randomly pick one of the six possible orientations with a corresponding probability, start the ℓ -step walk in that direction, and search whether all successive ℓ sites are unoccupied. If so, we occupy these $\ell + 1$ sites and deposit the object; otherwise, the deposition attempt is rejected. During the simulation of irreversible deposition we record the number of inaccessible sites in the lattice. A site is inaccessible if it is occupied or it cannot be the beginning of the shape. The jamming limit θ_{jam} is reached when the number of inaccessible sites is equal to the total number of lattice sites.

Mixtures of n line segments of various lengths are made of n k -mers starting from $k = 2$ to $k = n + 1$. The number of components is always increased by adding an object of a size greater for a lattice constant. For example, the two-component mixture of line segments consists of the line segments of length $\ell = 1$ and $\ell = 2$, the three-component mixture is made by adding a line segment of length $\ell = 3$, and so on. An n -component mixture contains line segments of length $\ell = 1, 2, \dots, n$. The irreversible RSA process for an n -component mixture is as follows. At each Monte Carlo step one of the n mixture components is chosen at random and one lattice site is selected at random. Then we try to deposit the k -mer with the beginning at the selected site in one of the six orientations chosen with a given probability. Again this probability is equal p or $(1 - p)/2$, depending on whether the randomly chosen direction is horizontal or not, respectively. We search whether the k consecutive sites in a chosen direction are unoccupied. If so, we occupy these k sites and place the k -mer. If not, the attempt is abandoned. Then a new site and a new depositing object from the mixture are selected at random, and so on. The jamming limit of the mixture θ_{jam} is reached when neither of the objects can be placed in any position on the lattice.

The Monte Carlo simulations are performed on a 2D triangular lattice of size $L = 128$. The time is counted by

the number of attempts to select a lattice site and scaled by the total number of lattice sites. Periodic boundary conditions are used in all directions. The data are averaged over 1000 independent runs for each depositing object as well as for the mixture. The finite-size effects, which are generally weak, can be neglected for object sizes $< L/8$ [16,40].

III. RESULTS AND DISCUSSION FOR SINGLE-COMPONENT SYSTEMS

First, we report and discuss the numerical results regarding the effects of anisotropy on deposition of k -mers on a 2D triangular lattice. The simulations have been performed for line segments of lengths $\ell = 1, 2, \dots, 10$. For all investigated k -mers and for all probabilities p of deposition in horizontal direction, plots of $\ln[\theta_{\text{jam}} - \theta(t)]$ versus t are straight lines for the late stages of deposition. These results are in agreement with the exponential approach to the jamming limit of the form (1) [15–18]. Furthermore, for a given probability p these plots are parallel lines in the late stages of the deposition process for k -mers of all lengths. This means that for a given degree of anisotropy, rapidity of the approach to the jamming state is not affected by the length of the k -mer. On the other hand, the degree of anisotropy has an essential influence in the late times of the deposition process.

Figure 1 shows the plots of $\ln[\theta_{\text{jam}} - \theta(t)]$ versus t for various values of the probability p for three k -mers of different lengths: (a) $k = 2$, (b) $k = 4$, and (c) $k = 10$. It can be seen that the slope of these lines in the late times of the process depends on probability p . It is observed that the slope of the line for a given probability $p \in (0, \frac{1}{3})$ is equal to the slope of the line corresponding to the probability $p' = 1 - 2p \in [\frac{1}{3}, 1)$. For example, the lines in Fig. 1 for probabilities 0.12 and 0.28 ($p < 1/3$) have the same slopes as lines corresponding to probabilities 0.76 and 0.44, respectively. Consequently, for an arbitrary value of probability $0 < p < 1$ for deposition in the horizontal direction, rapidity of the approach to the jamming state is determined by the value $p_0 = \min\{p, (1 - p/2)\}$, i.e., by the smallest value of probability for deposition in all three directions.

Our results suggest that the more prominent the anisotropy is, approach to the jamming limit is slower. To confirm this notion, we have calculated the values of the parameter σ from the slopes of the $\ln[\theta_{\text{jam}} - \theta(t)]$ versus t curves in the late times of the process. Parameter σ determines how fast the lattice is filled up to the jamming coverage θ_{jam} . The dependence of σ on the probability p is given in Fig. 2 for $k = 2, 3, 4, 6, 8,$ and 10. When p approaches unity or zero value, the value of parameter $p_0 = \min\{p, (1 - p/2)\}$ becomes very small, and the adsorption process slows down dramatically. In that case, large times are needed for filling of small isolated empty targets, left in the very late stages of deposition, if it can be filled by k -mers oriented only in direction corresponding to small probability p_0 . Reducing the probability p_0 , time needed to reach the jamming state may become arbitrarily large; i.e., relaxation time σ diverges to infinity when p_0 gets smaller. Numerical calculation of the parameter σ for cases of high anisotropy is difficult because it must be performed in vicinity of the vertical asymptote of the $\sigma(p)$ curve. Consequently, we have observed that the fluctuations of relaxation time σ

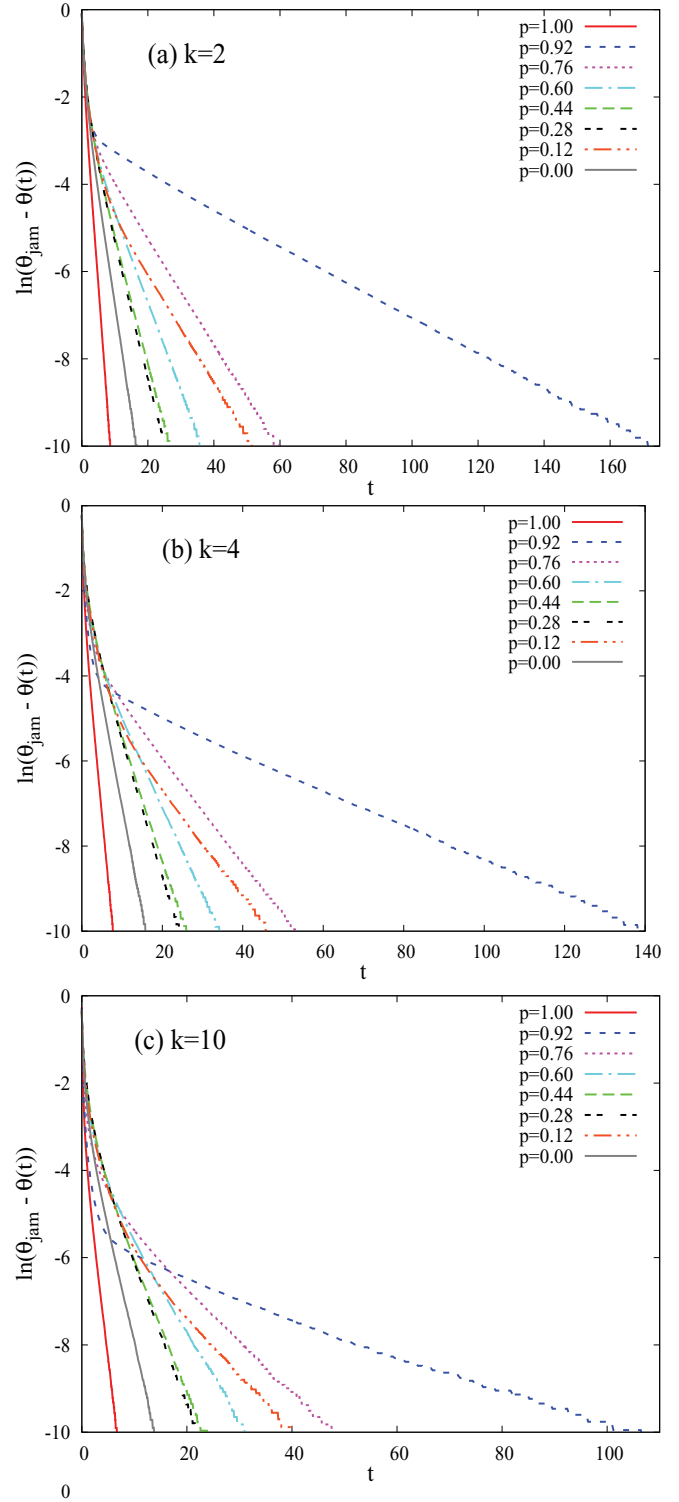


FIG. 1. (Color online) Plots of $\ln(\theta_{\text{jam}} - \theta(t))$ versus t for various probabilities p and for three different k -mers: (a) $k = 2$, (b) $k = 4$ and, (c) $k = 10$.

about the mean value increase with decreasing parameter p_0 , especially for large k -mers. It is numerically very expensive to sufficiently diminished statistical fluctuations associated with highly anisotropic conditions. Therefore, the relaxation times reported here are averages of 1000 independent simulations for each value of probability p . When p gets closer to

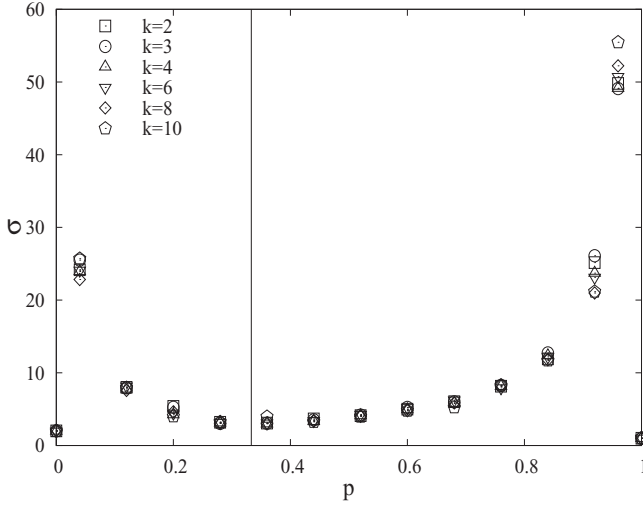


FIG. 2. Dependence of the parameter σ [Eq. (1)] on probability p for various k -mers. The vertical line indicates the value of $p = \frac{1}{3}$.

the value for the isotropic deposition ($p = \frac{1}{3}$), parameter σ decreases and reaches the value $\sigma \simeq 3.0$ for the isotropic case. In the case when adsorption is allowed only in one direction ($p = 1$), the process reduces to the one-dimensional case, and the corresponding value of parameter $\sigma \simeq 1.0$ is obtained [15,41]. When adsorption performs in two directions with equal probabilities ($p = 0$), dynamics is slower than for the one-dimensional case, but faster than even for the isotropic case, with $\sigma \simeq 2.0$.

Jamming coverage θ_{jam} also depends on the degree of anisotropy. From Fig. 3 we can see that this dependence differs for k -mers of various lengths. For $p = 1$ the one-dimensional results are obtained for all k -mers [42]. The RSA problem in one dimension is exactly solvable [3,41]. For k -mers, the jamming limit $\theta_{\text{jam}}(k)$ is given by [43]

$$\theta_{\text{jam}}(k) = \int_0^k du \exp \left[-2 \int_0^u dv \frac{1 - (1 - v/k)^{k-1}}{v} \right]. \quad (2)$$

From Eq. (2), a systematic derivation of the $1/k$ -Taylor expansion for the jamming coverage, $\theta_{\text{jam}}(k) = A_0 + A_1/k + A_2/k^2 + \dots$, is possible. Bartelt *et al.* [43] gave the explicit expressions and numerical values for the first three coefficients: $A_0 = 0.747598 \dots$, $A_1 = 0.216181 \dots$, $A_2 = 0.0362556 \dots$. From Fig. 3, we clearly observe that values of the jamming coverages $\theta_{\text{jam}}(k)$ calculated using Eq. (2) agree very well with the simulation results in one dimension ($p = 1$).

For all objects, the jamming coverage θ_{jam} exhibits a local minimum near $p = \frac{1}{3}$, i.e., for isotropic condition. For $k \geq 4$ this minimum is lower than the value of jamming coverage for deposition of k -mers in one dimension. However, the most striking feature is that a very small change in the probability p away from 0 or 1 brings an abrupt jump in the value of the jamming coverage θ_{jam} for the k -mers of small length ($k \leq 3$); e.g., when p changes from 0.96 to 1, the value of θ_{jam} for dimers drops from 0.92 to 0.86. The jump near $p = 0$ is smaller in magnitude. We now briefly explain the physical mechanism that underlies this behavior of jamming coverage. For p close to unity, when the adsorption in horizontal direction is much more efficient than in the other two, the configuration formed in

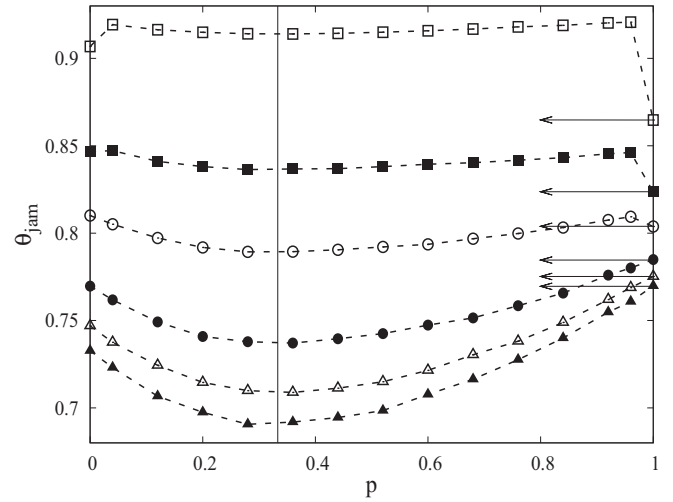


FIG. 3. Dependence of the jamming coverage θ_{jam} on probability p for various k -mers. The curves from top to bottom correspond to increasing values of $k = 2, 3, 4, 6, 8, 10$. The vertical line indicates the value of $p = \frac{1}{3}$. The horizontal arrows indicate values of the jamming coverages $\theta_{\text{jam}}(k)$ calculated using Eq. (2) for $k = 2, 3, 4, 6, 8, 10$, from top to bottom.

the long-time regime is made up of a large number of domains. In the case of the deposition of line segments, any such domain contains a large number of objects all close to each other and parallel. In the asymptotic regime, most new additions are inside the domains only, and a small number of additions take place if newly arriving objects are to be positioned in the interdomain spaces. Unlike the longer k -mers, for short k -mers there is an enhanced possibility for deposition into interdomain spaces when adsorption is allowed with a small probability in directions other than the privileged one. That is the reason why the jamming coverage of small line segments increases when p gets slightly lower than unity. When the depositing k -mers are longer, the possibility of adsorption in more different directions interferes with the tendency of their alignment, and the resulting jamming coverage has lower values. The same mechanism is responsible for the abrupt change of the jamming coverage at very low values of p , when the adsorption in horizontal direction is less favored than in the other two.

We also study the anisotropic irreversible deposition of objects of various shapes that can be made by self-avoiding random walks on a triangular lattice. At least two representative shapes of each order of symmetry $n_s \in \{1, 2, 3, 6\}$ are investigated. In the case of isotropic deposition ($p = \frac{1}{3}$), according to parameter σ (Eq. (1)), all extended shapes can be divided into four groups:

- Shapes with a symmetry axis of first order, $n_s = 1$, with $\sigma \simeq 5.9$
- Shapes with a symmetry axis of second order, $n_s = 2$, with $\sigma \simeq 3.0$
- Shapes with a symmetry axis of third order, $n_s = 3$, with $\sigma \simeq 2.0$
- Shapes with a symmetry axis of sixth order, $n_s = 6$, with $\sigma \simeq 0.99$.

This means that at late enough times, the rotational symmetries associated with specific shapes have a substantial influence on the adsorption rate of the objects. More symmetric

shapes reach their jamming coverage faster; i.e., the relaxation time σ is smaller for more symmetric objects. At large times, adsorption events take place on the islands of unoccupied sites. The individual islands act as selective targets for specific deposition events. In other words, there is only a restricted number of possible orientations in which an object can reach a vacant location, provided the location is small enough. For a shape of a higher order of symmetry n_s , there is a greater number of possible orientations for deposition into a selective target on the lattice. Hence, the increase of the order of symmetry of the shape enhances the rate of single-particle adsorption. This is reflected in the fact that the adsorption of asymmetric shapes is slower than the adsorption of more regular and symmetric shapes.

In the case of anisotropic deposition ($p \neq \frac{1}{3}$), for all investigated shapes and all probabilities of adsorption in a horizontal direction, plots of $\ln[\theta_{\text{jam}} - \theta(t)]$ versus t are straight lines in the late times of the process. Analyzing the results for a large number of various shapes, we can see that the kinetics of anisotropic deposition is determined mainly by the symmetry properties of the object. In order to illustrate how the deposition of various shapes is affected by the presence of anisotropy, we present the results of the simulations for one representative object of each order of symmetry, i.e., for 3-mer B, angled shape C, triangle D, and hexagon E shown in Table I. For these objects, dependence of the parameter σ on the probability p is given in Fig. 4. For the k -mer B covering three lattice sites and for the angled object C, rapidity of the approach to the jamming limit is affected by the presence of anisotropy. The dependence of the parameter σ on the probability p is more prominent for the less symmetric object C. For the values of p close to zero, the deposition process is very slow. The relaxation time σ decreases with p , reaches a minimum for the isotropic case, and increases for higher values of p . For the less symmetric object C, $\sigma \simeq 4.0$ for $p = 0$, and $\sigma \simeq 2.0$ for $p = 1$. For $p = \frac{1}{3}$, the expected result that $\sigma \simeq 6.0$ is obtained. Values of σ for the objects with symmetry axis of first order are twice higher than the corresponding values for

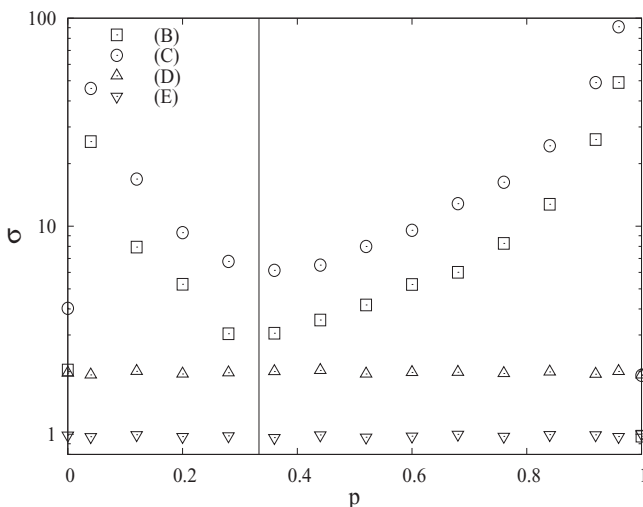


FIG. 4. Dependence of the parameter σ [Eq. (1)] on probability p for shapes B, C, D, and E from Table I. The vertical line indicates the value of $p = \frac{1}{3}$.

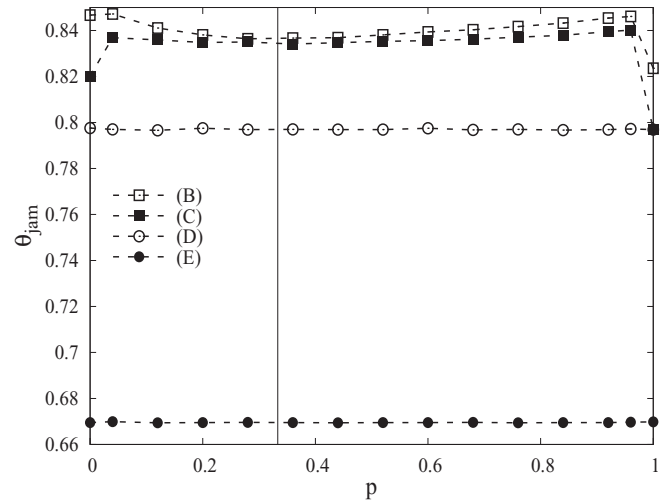
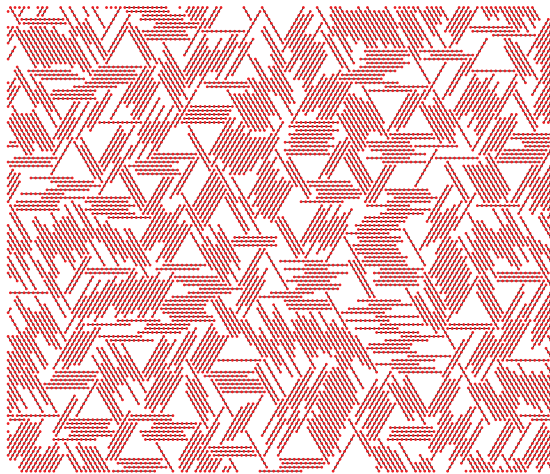


FIG. 5. Dependence of the jamming coverage θ_{jam} on probability p for shapes B, C, D, and E from Table I. The vertical line indicates the value of $p = \frac{1}{3}$.

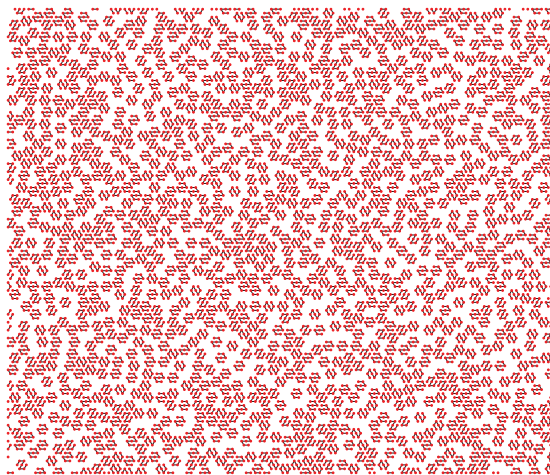
the objects with symmetry axis of second order for each value of the probability p . Deposition of the objects with symmetry axis of third and sixth order is not affected by the presence of anisotropy. No matter what the value of the probability p is, $\sigma \simeq 2.0$ for the objects with symmetry axis of third order, and $\sigma \simeq 1.0$ for the objects with symmetry axis of sixth order.

As one can see from Fig. 5, the jamming coverage depends on the probability p for the shapes with symmetry axis of first and second order. On the contrary, for the objects with symmetry axis of third and sixth order, the values of θ_{jam} do not depend on p , and the isotropic values of jamming coverages are obtained [31]. At very early times of the process the depositing objects do not “feel” the presence of the already deposited ones and are placed randomly onto the lattice. However, in the late stages of deposition the objects must fit into small empty regions that favors the formation of clusters. Line segments and angled shapes deposited in the late stages of deposition must deposit parallel to the already deposited ones in order to avoid an intersection. This is reflected in the relatively high local packing of nearly parallel adsorbed objects in the vicinity of given object in the case of line segments and angled objects as compared to the triangles and hexagons. Such a different object view is the cause of the enhanced growth of very compact domains in the case of elongated shapes as compared to those in the case of more round (symmetric) shapes, resulting in a higher value of the jamming coverage fraction in the former case.

In Fig. 6 we compare the geometric status of the representative snapshots of patterns formed during the RSA of k -mers ($k = 10$) and hexagons E for the isotropic case ($p = \frac{1}{3}$). The mesh structure of the open spaces look very different for adsorbing k -mers or hexagons E. The jamming configuration for k -mers consists of domains of parallel lines and large clusters of blocked sites [44]. If the depositing objects are highly symmetrical there are also clusters of blocked sites in the jamming configurations, but their sizes are smaller. It must be stressed that for highly symmetric objects, the presence of anisotropic conditions do not influence both the



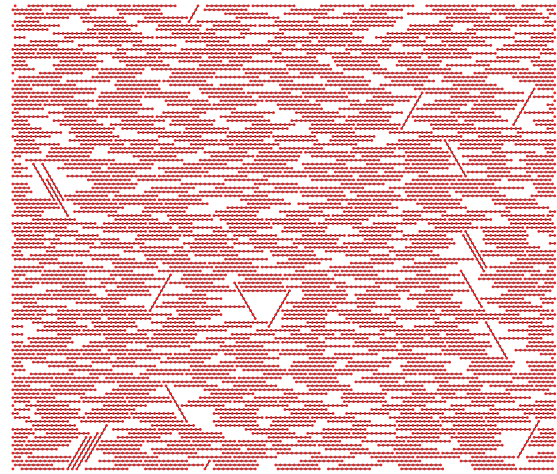
(a)



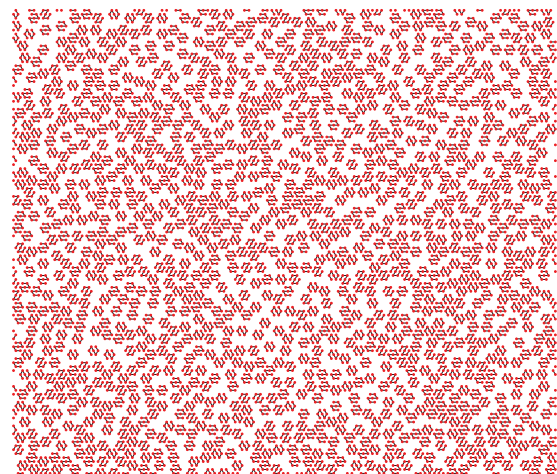
(b)

FIG. 6. (Color online) Snapshots of patterns formed during the RSA of (a) k -mer ($k = 10$), and (b) hexagon E correspond to jamming state for the isotropic case, $p = \frac{1}{3}$.

value of relaxation time σ and the value of jamming coverage θ_{jam} . For regular objects, such as hexagon E, all islands of unoccupied sites on lattice can be treated as nonselective targets for deposition events. Indeed, if a highly symmetric object is placed on vacant locations, it can be freely rotated about its symmetry axis, regardless of the size and shape of a given target. Therefore, the presence of a privileged direction for deposition has no influence on the placement of highly symmetric objects on the lattice. That this is so can be seen from Fig. 7, which shows typical jamming configurations for the deposition of k -mers ($k = 10$) and hexagons E in the presence of anisotropy ($p = 0.92$). Evidently, patterns formed during the anisotropic RSA of k -mers show a deposition-induced horizontal alignment. This geometry admits of a high coverage limit. However, if we compare the two snapshots of patterns formed during the isotropic [Fig. 6(b)] and anisotropic [Fig. 7(b)] deposition of hexagons, the structure of clusters of blocked sites does not appear too different for the eye.



(a)



(b)

FIG. 7. (Color online) Snapshots of patterns formed during the RSA of (a) k -mer ($k = 10$), and (b) hexagon E correspond to jamming state for the case of $p = 0.92$.

IV. DEPOSITION OF POLYDISPERSE MIXTURES IN ANISOTROPIC CONDITIONS

As an example of a polydisperse mixture, a 10-component mixture of line segments of lengths $\ell = 1, 2, \dots, 10$ is studied. Kinetics of the irreversible deposition of this mixture is illustrated in Fig. 8, where the plots of $\ln[\theta_{\text{jam}} - \theta(t)]$ versus t are given for the various probabilities p of deposition in horizontal direction. It was found that for all probabilities p , these plots are straight lines for the late stages of the deposition process, not only for the mixtures, but also for each of the components (not shown here). This means that the exponential temporal evolution (1) of the coverage $\theta(t)$ is valid for all p both for the mixture and for the components making the mixture. As for the pure lattice shapes, the late-stage deposition kinetics is strongly influenced by the presence of anisotropy.

The dependence of the relaxation time σ on the probability p for the 10-component mixture of k -mers is given in Fig. 9. For the values of p close to zero or unity, the deposition process is very slow. The parameter σ reaches a local minimum for the isotropic case. For $p = 1$ the one-dimensional result for the

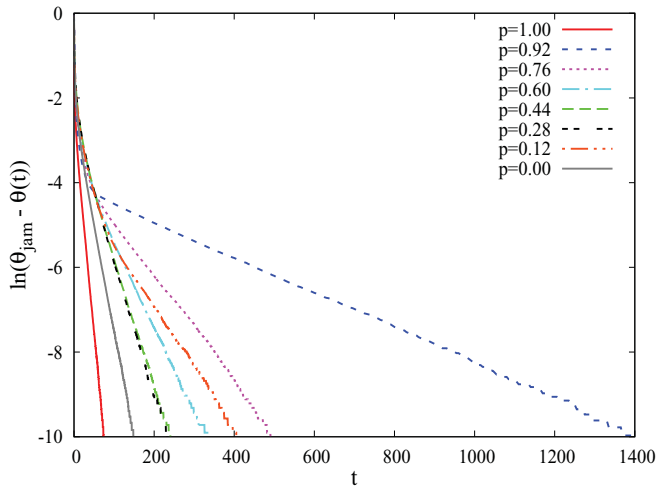


FIG. 8. (Color online) Plots of $\ln[\theta_{\text{jam}} - \theta(t)]$ versus t for the 10-component mixture of k -mers ($k = 2, 3, \dots, 11$) for various probabilities p .

10-component mixture is obtained [34]. Comparing the results from Fig. 2 and Fig. 9, we can see that for a given degree of anisotropy, the parameter σ for a mixture is always greater than either of the relaxation times for the k -mers of length $\ell = 1, 2, \dots, 10$.

Values of the total jamming coverage θ_{jam} for the 10-component mixture of k -mers are given in Fig. 10 for various values of probability p . It is important to note that arbitrary mixtures cover the lattice more efficiently than either of the components. The reason for this property of polydisperse mixtures has been discussed in detail in previous papers [18,34]. The minimal value obtained for the isotropic case is lower than the values for $p = 0$ and 1. The jamming coverage increases when the degree of anisotropy increases, because the alignment of long components of the mixture in the early stage of the process leads to more efficient densification afterward.

Figure 11 gives an additional insight into the kinetics of the mixture components. Values of the relaxation times σ for the

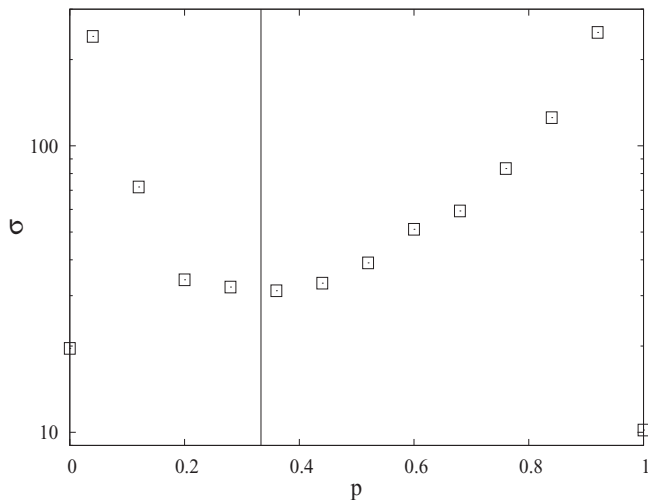


FIG. 9. Dependence of the parameter σ [Eq. (1)] on probability p for the 10-component mixture of k -mers ($k = 2, 3, \dots, 11$). The vertical line indicates the value of $p = \frac{1}{3}$.

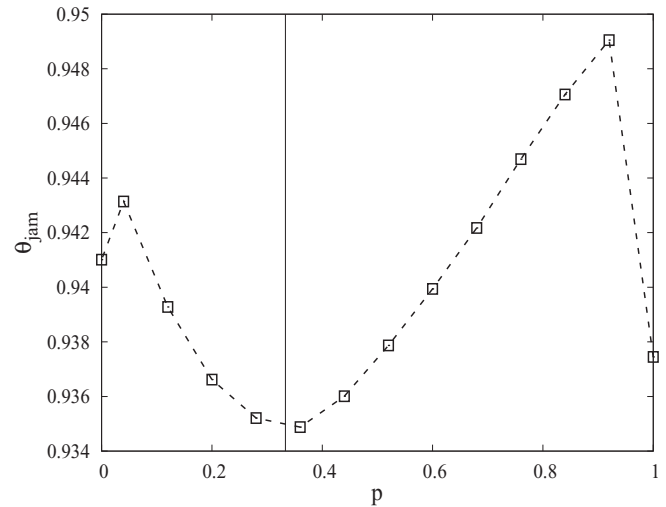


FIG. 10. Dependence of the total jamming coverage θ_{jam} on probability p for the 10-component mixture of k -mers ($k = 2, 3, \dots, 11$). The vertical line indicates the value of $p = \frac{1}{3}$.

line segments of length $\ell = 1, \dots, 10$ making a 10-component mixture are shown for $p = 0.84$ and for the isotropic case, $p = \frac{1}{3}$. In both cases, the relaxation time σ decreases rapidly with the length of the components making the mixture. It is intuitively clear that in the late times the kinetics of the deposition is determined mostly by the smallest objects in the mixture. Every occupation by the smaller object creates an exclusion zone for further adsorption of larger objects. At large times, adsorption events take place on small domains of unoccupied sites, and in the competition for the deposition between two objects of a different number of segments the smaller object wins. Furthermore, in the presence of anisotropy, adsorption of shorter k -mers slows in comparison to the isotropic case. In other words, presence of anisotropy favors the adsorption of longer objects. This conclusion is consistent with the numerical results plotted in Fig. 12. For all probabilities p , partial jamming coverage decreases with

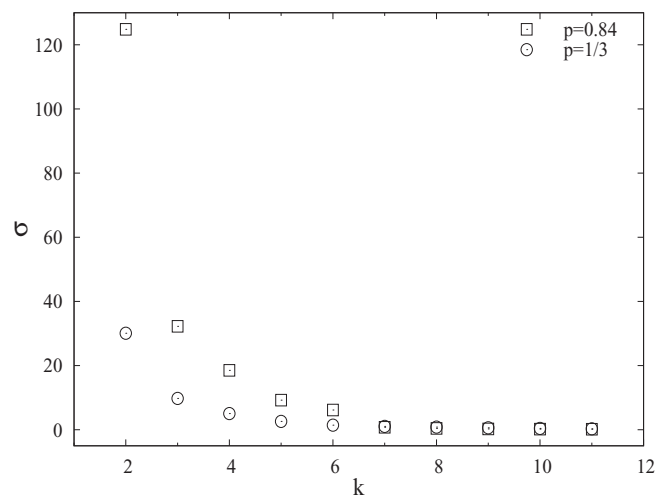


FIG. 11. Values of the parameter σ [Eq. (1)] for the k -mers, $k = 2, 3, \dots, 11$, making a 10-component mixture for the case of $p = 0.84$ and for the isotropic case, $p = \frac{1}{3}$.

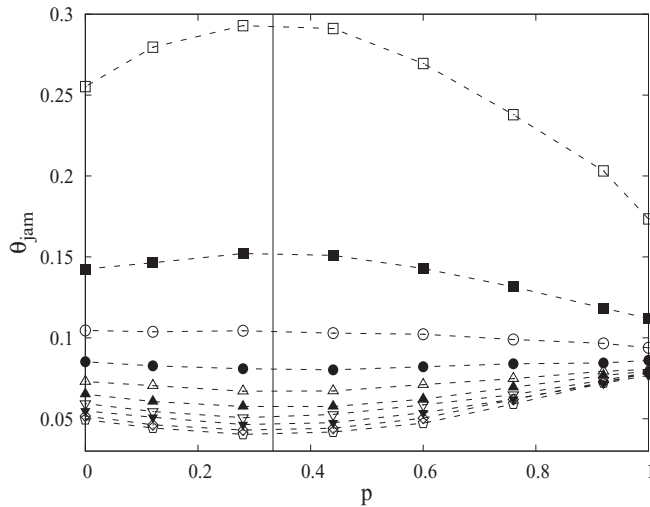


FIG. 12. Dependence of partial jamming coverages θ_{jam} on probability p for k -mers making a 10-component mixture. The curves from top to bottom correspond to increasing values of $k = 2, 3, \dots, 11$. The vertical line indicates the value of $p = \frac{1}{3}$.

the length of k -mers. These changes are most pronounced for the case of isotropic deposition. For short k -mers ($k \leq 4$), partial jamming coverages increase with p , reach a maximum for the isotropic condition, and decrease for higher values of p . However, partial jamming coverages of longer k -mers ($k \geq 5$) exhibit a shallow minimum near $p = \frac{1}{3}$. Hence, our results suggest that anisotropic constraints lead to decreased (increased) contribution of the short (long) k -mers in the total coverage fraction.

V. CONCLUDING REMARKS

We have investigated numerically the effect of anisotropy on the RSA of extended objects on a planar triangular lattice. A systematic approach is made by using the objects of different number of segments and rotational symmetries. We have also presented the numerical results of anisotropic RSA for multicomponent mixtures of k -mers.

It was shown that the growth of the coverage $\theta(t)$ to the jamming limit θ_{jam} occurs via the exponential law (1), for all the shapes and mixtures considered and for all values of probability p of deposition in a preferential direction. The simulations have shown that the kinetics of anisotropic deposition is determined mainly by the symmetry properties of the object. In the case of elongated and asymmetrical shapes, the relaxation time σ is found to increase with the degree of

anisotropy. However, for rounded and symmetrical shapes, rapidity of the approach to the jamming state is not affected by the presence of anisotropy. A similar qualitative behavior of the jamming limit θ_{jam} in anisotropic condition is obtained; for highly symmetric objects, no dependence of the jamming coverage θ_{jam} on the probability p is observed within the statistical uncertainties. Nevertheless, the jamming coverage depends on the probability p for the shapes with lower-order symmetry axis.

We have analyzed the polydisperse mixtures in which the size of line segments making the mixture gradually increases with the number of components. Also, we have performed a detailed analysis of the contribution to the densification kinetics coming from each mixture component. Strong dependencies both of the value of relaxation time σ and of the jamming coverage θ_{jam} on the degree of anisotropy are obtained. The value of σ has larger values for a mixture than for the pure shapes for all probabilities p , so we can generally say that the deposition process is always slower for a mixture than for the pure shapes making the mixture. Furthermore, the jamming coverage for a mixture of line segments is greater than either of the jamming coverages of the components making the mixture, regardless of the degree of anisotropy. It is found that anisotropic constraints lead to the increased contribution of the longer k -mers in the total coverage fraction of the mixture.

Recently we have performed extensive numerical simulation of the RSA on triangular lattice using polydisperse mixtures in which the size of extended shapes making the mixture gradually increases with number of components n [18]. We showed that for the mixtures of more symmetric shapes, such as line segments and triangles, jamming coverage increases with n , contrary to the mixture of angled shapes where jamming coverage decreases. These results suggest that the order of symmetry axis of the shape may exert a decisive influence on the adsorption efficiency of polydisperse mixture in isotropic conditions. The presented numerical analysis could be a first step toward studying more complex systems, such as the case of anisotropic RSA of polydisperse mixtures of extended objects and mixtures of arbitrarily chosen self-avoiding random-walk chains.

ACKNOWLEDGMENTS

This work was supported by the Ministry of Science of the Republic of Serbia, Grants Nos. ON171017 and III45016. The work was also supported by the Swiss National Science Foundation through the SCOPES grant IZ73Z0-128169. We would like to thank Professor V. Privman for helpful discussions.

- [1] V. Privman, ed., *Nonequilibrium Statistical Mechanics in One Dimension* (Cambridge University Press, Cambridge, UK, 1997) (a collection of review articles).
- [2] V. Privman, ed., *Colloids Surf. A* **165**, 1 (2000) (a collection of review articles).
- [3] J. W. Evans, *Rev. Mod. Phys.* **65**, 1281 (1993).
- [4] A. Cadilhe, N. A. M. Araújo, and V. Privman, *J. Phys. Condens. Matter* **19**, 065124 (2007).

- [5] V. V. Tsukruk, H. Ko, and S. Peleshanko, *Phys. Rev. Lett.* **92**, 065502 (2004).
- [6] B. S. Shim and N. A. Kotov, *Langmuir* **21**, 9381 (2005).
- [7] C. Park, J. Wilkinson, S. Banda, Z. Ounaies, K. E. Wise, G. Sauti, P. T. Lillehei, and J. S. Harrison, *J. Polym. Sci. B: Polym. Phys.* **44**, 1751 (2006).
- [8] V. G. Cheung, M. Morley, F. Aguilar, A. Massimi, R. Kucherlapati, and G. Childs, *Nat. Genet.* **21**, 15 (1999).

- [9] X. Gao, E. LeProust, H. Zhang, O. Srivannavit, E. Gulari, P. Yu, C. Nishiguchi, Q. Xiang, and X. Zhou, *Nucl. Acids Res.* **29**, 4744 (2001).
- [10] R. Erban and S. J. Chapman, *J. Stat. Phys.* **127**, 1255 (2007).
- [11] J. Feder, *J. Theoret. Biol.* **87**, 237 (1980).
- [12] R. H. Swendsen, *Phys. Rev. A* **24**, 504 (1981).
- [13] Y. Pomeau, *J. Phys. A* **13**, L193 (1980).
- [14] B. Bonnier, *Phys. Rev. E* **64**, 066111 (2001).
- [15] M. C. Bartelt and V. Privman, *J. Chem. Phys.* **93**, 6820 (1990).
- [16] S. S. Manna and N. M. Švrakić, *J. Phys. A* **24**, L671 (1991).
- [17] Lj. Budinski-Petković and U. Kozmidis-Luburić, *Phys. Rev. E* **56**, 6904 (1997).
- [18] Lj. Budinski-Petković, S. B. Vrhovac, and I. Lončarević, *Phys. Rev. E* **78**, 061603 (2008).
- [19] M. J. de Oliveira, T. Tomé, and R. Dickman, *Phys. Rev. A* **46**, 6294 (1992).
- [20] V. A. Cherkasova, Y. Y. Tarasevich, N. I. Lebovka, and N. V. Vygornitskii, *Eur. Phys. J. B* **74**, 205 (2010).
- [21] F. Du, J. E. Fischer, and K. I. Winey, *Phys. Rev. B* **72**, 121404 (2005).
- [22] J. D. Sherwood, *J. Phys. A* **23**, 2827 (1990).
- [23] B. J. Brosilow, R. M. Ziff, and R. D. Vigil, *Phys. Rev. A* **43**, 631 (1991).
- [24] P. Viot, G. Tarjus, S. M. Ricci, and J. Talbot, *J. Chem. Phys.* **97**, 5212 (1992).
- [25] Z. Adamczyk and P. Weron, *J. Chem. Phys.* **105**, 5562 (1996).
- [26] J. Talbot, G. Tarjus, P. R. Van Tassel, and P. Viot, *Colloids Surfaces A* **165**, 287 (2000).
- [27] R. D. Vigil and R. M. Ziff, *J. Chem. Phys.* **91**, 2599 (1989).
- [28] G. C. Barker and M. J. Gimson, *Mol. Phys.* **63**, 145 (1988).
- [29] P. Meakin and R. Jullien, *Phys. Rev. A* **46**, 2029 (1992).
- [30] B. Bonnier, Y. Leroyer, and E. Pommiers, *J. Phys. I* **2**, 379 (1992).
- [31] I. Lončarević, Lj. Budinski-Petković, and S. B. Vrhovac, *Eur. Phys. J. E* **24**, 19 (2007).
- [32] Z. Adamczyk, B. Siwek, M. Zembala, and P. Weron, *J. Colloid Interface Sci.* **185**, 236 (1997).
- [33] N. V. Brilliantov, Y. A. Andrienko, P. L. Krapivsky, and J. Kurths, *Phys. Rev. Lett.* **76**, 4058 (1996).
- [34] I. Lončarević, Lj. Budinski-Petković, S. B. Vrhovac, and A. Belić, *J. Stat. Mech.: Theor. Exp.* (2010) P02022.
- [35] J. Talbot and P. Schaaf, *Phys. Rev. A* **40**, 422 (1989).
- [36] M. C. Bartelt and V. Privman, *Phys. Rev. A* **44**, R2227 (1991).
- [37] G. Tarjus and J. Talbot, *Phys. Rev. A* **45**, 4162 (1992).
- [38] P. L. Krapivsky, *J. Stat. Phys.* **69**, 135 (1992).
- [39] N. A. M. Araújo and A. Cadilhe, *Phys. Rev. E* **73**, 051602 (2006).
- [40] M. Nakamura, *Phys. Rev. A* **36**, 2384 (1987).
- [41] M. C. Bartelt and V. Privman, *Int. J. Mod. Phys. B* **5**, 2883 (1991).
- [42] G. J. Rodgers, *Phys. Rev. E* **48**, 4271 (1993).
- [43] M. C. Bartelt, J. W. Evans, and M. L. Glasser, *J. Chem. Phys.* **99**, 1438 (1993).
- [44] R. M. Ziff and R. D. Vigil, *J. Phys. A: Math. Gen.* **23**, 5103 (1990).